17th World Conference on Earthquake Engineering, 17WCEE
Sendai, Japan - September 13th to 18th 2020

Variation evaluation of path and site amplification characteristics using Fourier amplitude spectral ratio

Y. Fukushima[(1)], T. Nagao[(2)]

[(1)] *Senior Engineer, Eight-Japan Engineering Consultants Inc., Okayama, Japan, E-mail: fukushima-ya@ej-hds.co.jp*
[(2)] *Professor, Research Center for Urban Safety and Security, Kobe University, Kobe, Japan, nagao@people.kobe-u.ac.jp*

Abstract

Since earthquake ground motions have a randomness, it is necessary to evaluate variations of earthquake ground motions for earthquake engineering practice such as seismic hazard analysis, risk analysis, and earthquake resistant structural design. Earthquake ground motions can be expressed by using source, path and site amplification characteristics. Site amplification characteristic implies an amplification factor in the frequency domain due to the deep and shallow subsurface condition. Site amplification characteristic greatly differs from site to site, because the amplification characteristics is affected by the three-dimensional sedimentary environment of soil layers. Path characteristic implies an attenuation characteristics and it also varies for different sites.

Six earthquake ground motion observation stations in Fukushima and Ibaraki Prefectures in Japan were picked up for the study. Spectral ratio of strong motion records at two sites by the same event can be regarded as the ratio of the multiplication of path and site amplification characteristic. By considering the theoretical path spectra and empirically obtained quality factor and site amplification factors, spectral ratios of the strong motion records were obtained. The evaluated spectral ratios were consistent with the previous studies, showing average standard deviations varying from 0.176 to 0.244 at frequencies from 0.2 to 5.0 Hz.

It was found that the longer the distance between the two sites was, the larger the variation of the spectral ratios tended to be. A conceivable explanation is that the effect by the variation in path characteristic becomes non-negligible when the distance between the two sites becomes large. Therefore, another data set with almost the same hypocentral distances for the two sites were provided, and the change in the standard deviations of the spectral ratios were examined.

Keywords: earthquake ground motion, site amplification factor, path characteristic, Fourier spectrum

1. Introduction

It is very important to evaluate the variation of earthquake ground motion in hazard analysis, risk analysis, and seismic design of structures. Since earthquake ground motion can be expressed by source, path, and site characteristics [1], it is necessary to discuss the variations of the three characteristics individually when examining the dispersion of earthquake ground motions. Of the three characteristics, site amplification characteristics are amplification factors by deep and shallow subsurface, and it is known that they differ greatly from site to site. Although only amplification by shallow subsurface is often discussed as site amplification characteristics, in this study, amplification characteristics by deep subsurface which has a dominant effect along with the amplification by the shallow subsurface are examined and referred to as a site amplification factor. In other words, site amplification factor considered in this study is the amplification of the seismic motion at the ground surface with respect to the seismic bedrock for each frequency. There are two methods for evaluating the site amplification factor based on strong motion records: spectral inversion methods [e.g., 2, 3] and spectral ratio analysis observed at two neighboring sites. The average site amplification factors were the major subject of discussion in the literature, and dispersion of the site amplification factors has been hardly discussed. Regarding path characteristics, it has been pointed out that Q-values representing inelastic attenuation differ depending on the region [e.g., 4], but there has been little discussion on the dispersion of path characteristics.

Fukushima and Nagao [5] calculated the site amplification factor of the target site for a large number of earthquakes by multiplying the strong-motion Fourier spectral ratio of the target site to the reference site by the product of theoretical path spectral ratio and the empirical site amplification spectra at the reference site. The results show that the longer the distance between the reference and target point, the greater the site amplification factor variation tends to be. As the reason, it was suggested that the effect of the fluctuation of the propagation path characteristic increases when the distance between the reference and target point is large. It should be noted that the "site amplification factor" determined by the spectral ratio of the observation records at two sites is actually the ratio of the product of site amplification and path spectra, and therefore, the "site amplification factor dispersion" evaluated in previous studies is actually the dispersion of the product of path and site amplification factor ratio (PSR).

In this study, PSRs were calculated on the basis of the spectral ratios of the observed records as in Fukushima and Nagao [5] (Fig.1), and the dispersion of PSR was evaluated. The relationship between the dispersion of PSRs and the distance between the reference and target sites are discussed.

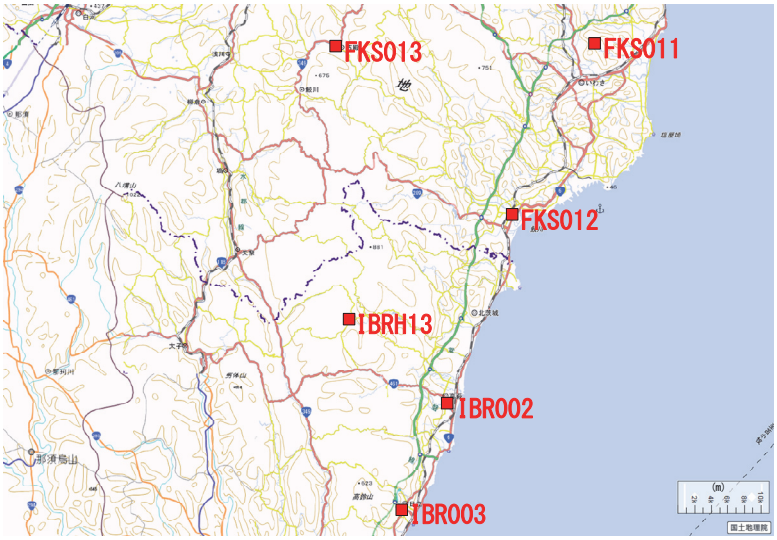

Fig. 1 – Study target (added to the Geospatial Information Authority of Japan's map)

2. Evaluation Method of PSR

Let T denote the target site and R denote the reference site at which the site amplification factor is known. The Fourier amplitude spectra $O_R(f)$ and $O_T(f)$ of the observed records at both sites can be expressed as the product of source characteristics $S(f)$, path characteristics $P_R(f)$, $P_T(f)$, and site amplification factor $G_R(f)$, $G_T(f)$ by the following formula.

$$O_R(f) = S(f) \cdot P_R(f) \cdot G_R(f) \tag{1}$$

$$O_T(f) = S(f) \cdot P_T(f) \cdot G_T(f) \tag{2}$$

Here, the theoretical expressions for the path characteristics $P_R(f)$ and $P_T(f)$ are expressed as

$$P_R(f) = \exp\{-(\pi f r_R)/(Q(f)V_S)\}/r_R \tag{3}$$

$$P_T(f) = \exp\{-(\pi f r_T)/(Q(f)V_S)\}/r_T \tag{4}$$

where r_R, r_T is the hypocentral distance to points R and T, V_S is the S-wave velocity, and $Q(f)$ is the Q-value representing the inelastic damping of the propagation path. Referring to the Q-value for East Japan Trench-type earthquake in Sato and Tatsumi [6], which is also used in the spectral inversion of the Nozu and Nagao 2), Equation [5] is used here.

$$Q(f) = 114 f^{0.92} \tag{5}$$

PSR can hence be expressed by:

$$PSR = \frac{O_T(f)}{O_R(f)} \times \frac{P_R(f) \cdot G_R(f)}{P_T(f) \cdot G_T(f)} \tag{6}$$

Here, we use site amplification factor $G_R(f)$ and $G_T(f)$ obtained by Nozu and Nagao [2] using spectral inversion.

In this paper, we evaluate the dispersion of PSR. The final target is the dispersion evaluation of site amplification and path spectra, but the method applied in this study cannot separate the site amplification and path characterisitics. In addition, the use of Q-values and site amplification factor from previous studies in the calculation of PSRs does not preclude the inclusion of variability in PSRs from those proposed in previous studies.

Strong motion records of small earthquakes are often of not good S/N ratio at low frequencies, and strong motion records of large earthquakes are affected by the rupture process of source faults, so that strong motion records of earthquakes of M_J 4.5 to less than 6.0 are targeted. Of the simultaneous observation records between the target and reference point, records having good S/N ratios down to 0.2 Hz from the viewpoint of compatibility with the ω^{-2} law [7] are used. In addition, in order to eliminate the effect of shallow subsurface nonlinearity, strong motion records with maximum accelerations of less than 1 m/s^2 were used, and strong motion records with epicentral distances of less than 150 km were used to avoid the effect of surface waves originating from the source.

The observed spectra were taken as 163.84 seconds of 100 Hz sampling and smoothed by a Parzen window with a bandwidth of 0.2 Hz. To eliminate the influence of radiation patterns, the square root of the sum of squares of the mean horizontal two components is used.

3. Dispersion of PSR

3.1 Reference and target site

Similar to Fukushima and Nagao [5], six K-NET [8], KiK-net [9] strong-motion seismograph stations in Fukushima and Ibaraki Prefectures shown in Fig.1 are targeted. Fig.2 shows the site amplification factors of the six targeted sites obtained by spectral inversion. For each station, the number of seismograms used for spectral inversion is 51 for FKS011, 56 for FKS012, 66 for FKS013, 83 for IBR002, 74 for IBR003, and 17 for IBRH13. In contrast to the large amplification factors in the frequency band below 1 Hz for FKS011, FKS012, and IBR002, the amplification factors at 1 Hz or less in FKS013, IBR003, and IBRH13 are small and have peaks in the high frequency region above 2.5 Hz. This difference in low-frequency site amplification factors reflects the difference in sedimentary environments at each location. The relation between the sediment thickness and the mean site amplification factor of 0.2-1 Hz is shown in Fig.3. Here, the sediment thickness is taken as the depth in the seismic bedrock of shear-wave velocity 3 km/s or more, referring to the values in the "Seismic Hazard Station J-SHIS" [10]. Higher correlations are found between the deposited layer thickness and the mean site amplification factor. In other words, the more thick the deposition layer, the smaller the predominant frequency in the site amplification factor.

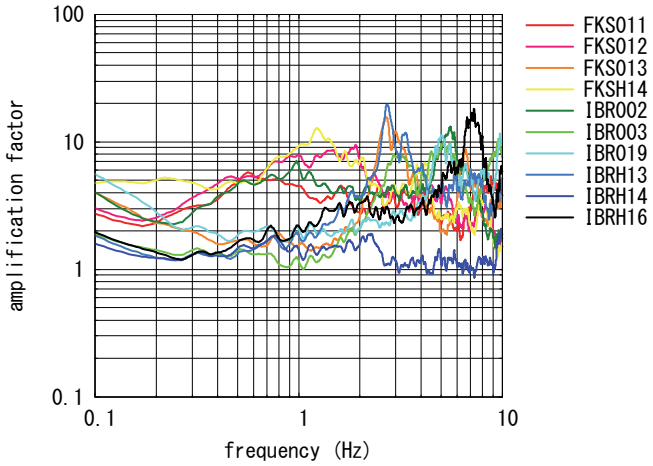

Fig. 2 – Site amplification factors obtained by spectral inversion

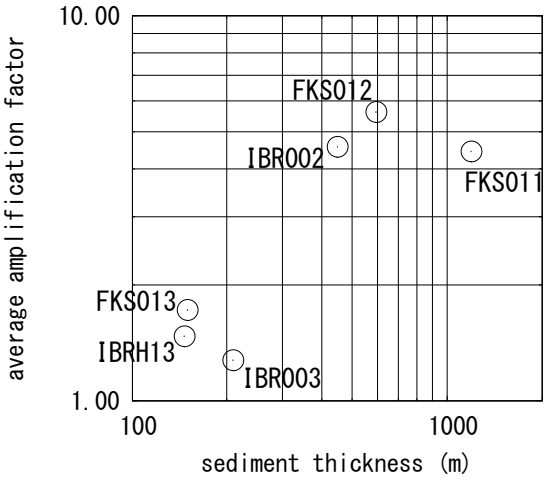

Fig. 3 – Relationships between sediment thickness and site amplification factor averages of 0.2 to 1 Hz

3.2 Calculation of PSR

PSR was calculated for the six locations shown in Fig.1. Table 1 shows the number of records of simultaneous observations at the reference and target point used for the examination. Case 1 in the table is a case in which no constraint was posed on the selection of the target seismogram, and Case 2 is a case in which a constraint was posed on the selection of the target seismogram, the details will be described later.

Table 1 – Number of strong-motion records used in the study (Upper: Case 1, Lower: Case 2)

		R:					
		FKS011	FKS012	FKS013	IBR002	IBR003	IBRH13
T:	FKS011		334	237	310	194	159
			62	35	35	15	21
	FKS012	334		276	378	235	185
		62		105	74	33	47
	FKS013	237	276		265	173	134
		35	105		60	18	39
	IBR002	310	378	265		266	198
		35	74	60		113	130
	IBR003	194	235	173	266		142
		15	33	18	113		65
	IBRH13	159	185	134	198	142	
		21	47	39	130	65	

As an example of PSRs, Fig.4 shows the results when IBR003 is taken as point *T*. The blue line in the figure is Case 1, the green line is Case 2, the solid line denotes the average value, and the dotted line expresses the average ± standard deviation. The average is the geometric mean on the common logarithmic axis, and the standard deviation is also calculated on the common logarithmic axis. PSR is unity when path and site amplification characteristics have no variations and correctly evaluated. However, focusing on the results in Case 1, PSR is approximately 1.0 or less when the reference point is IBR002, whereas peak and dip are observed particularly in the high frequency range of about 3 Hz or more when the reference point is FKS011 or FKS013, which is approximately five times the value at the maximum.

3.3 Relationship between reference and target point distance and dispersion of PSR

The relationship between the reference and target point distance and the average standard deviation of PSR in the frequency band of 0.2-5.0 Hz is shown in Fig.5. This frequency band is determined considering that both the S/N ratio of the earthquake record used in this study and accuracy of site amplification factor by Nozu and Nagao [2] is confirmed down to 0.2 Hz and by considering that the critical frequency band of civil engineering structures in the seismic design is generally up to 5 Hz (for example, highway bridges have natural periods of 0.3 second or more [11]). As in Fukushima and Nagao [5], the standard deviation of the PSR tends to increase as the reference and target point distance increases. As described above, Fukushima and Nagao [5] pointed out the possibility that if the reference and target point distance is large, the effect of the variation of the path characteristics increases.

The theoretical path spectra assumes geometric attenuation characteristic as inversely proportional to the hypocentral distance as shown in Eq. (3) to (4), but some claims that evaluated geometric attenuation does not necessarily inversely proportional to the hypocentral distance [e.g., 12]. Also, it has been pointed out that the Q-value differs from region to region [4].

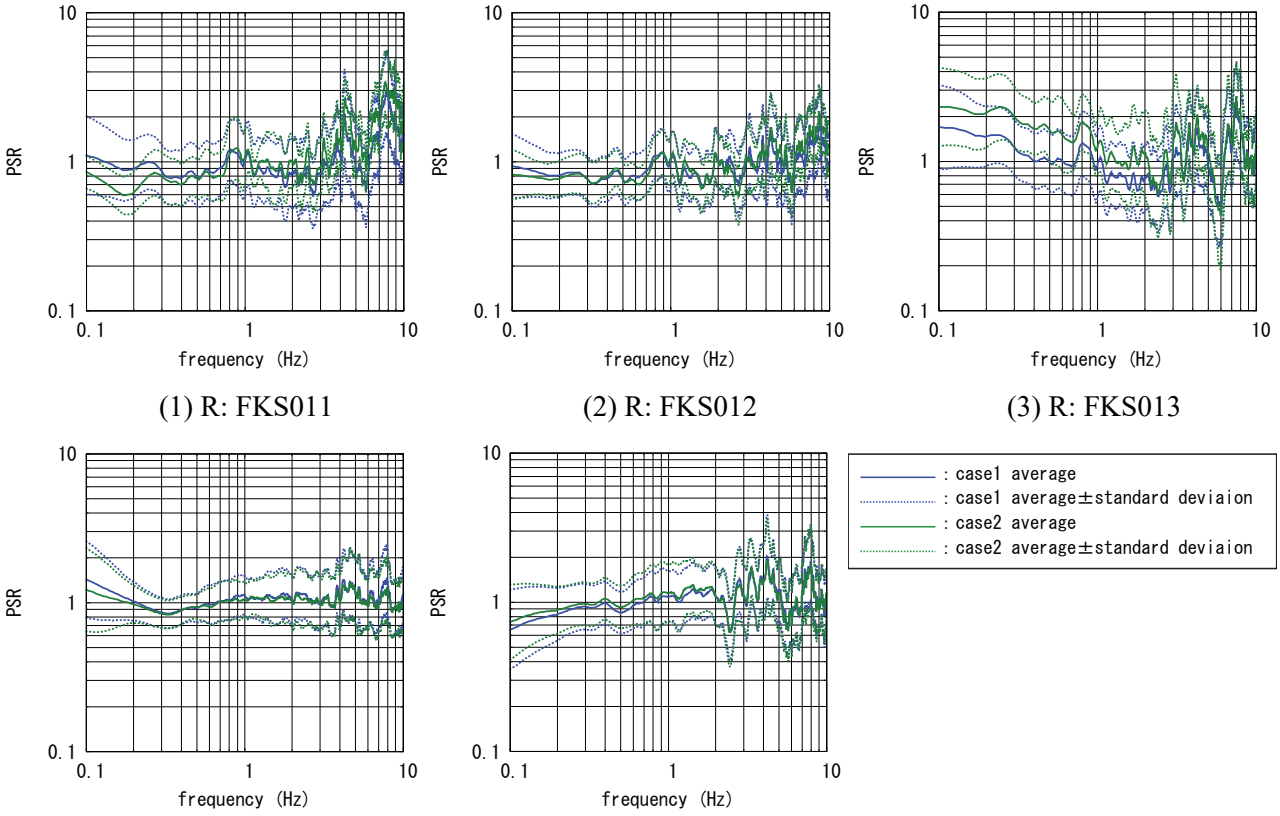

(1) R: FKS011 (2) R: FKS012 (3) R: FKS013

(4) R: IBR002 (5) R: IBRH13

Fig. 4 – PSRs with IBR003 as Point T

If the reason of the increase in dispersion of PSRs along with the increase in the site distance is attributed to the difference in the path characteristic between the sites, the dispersion of the PSR may not depend on the reference and target points distance if we only use seismograms whose hypocentral distance differences between the reference and target sites are negligible. From such a viewpoint, the scatter was reevaluated by limiting the data in which the hypocentral distance difference to the reference and target point is 10% or less (Case 2). The relationship between the reference and target point distance and the average standard deviation of PSR at 0.5 to 5 Hz is shown in Fig.6. Compared with Case 1 in Fig.5, cases with target sites IBR002 and IBRH13 have higher correlation between the site distance and the standard deviation of PSR, while others have lower correlation. There are combinations in which the dispersion decreases remarkably in Case 2 (e.g. cases of T: FKS011 - R: IBR003, T: FKS012 - R: IBRH13, T: IBR003 - R: FKS011, and T: IBRH13 - R: FKS012). The significant decrease in standard deviation in some combinations by limiting the hypocentral distance to the same extent may suggest the reason of the increase in the dispersion of PSR for cases with long sites distances as other than the difference between points in geometric attenuation characteristics. Other factors affecting the dispersion of PSR would be: (i) hypocenter-to-station azimuth: amplification factor changes due to differences in propagation paths [e.g., 13], (ii) incident angle of earthquake ground motion: amplification factor tends to increase as the incident angle increases [e.g., 14], (iii) basin-induced surface wave: amplification factor increases due to the generation of basin-induced surface wave [e.g., 2], etc. Therefore it is necessary to examine them in the future.

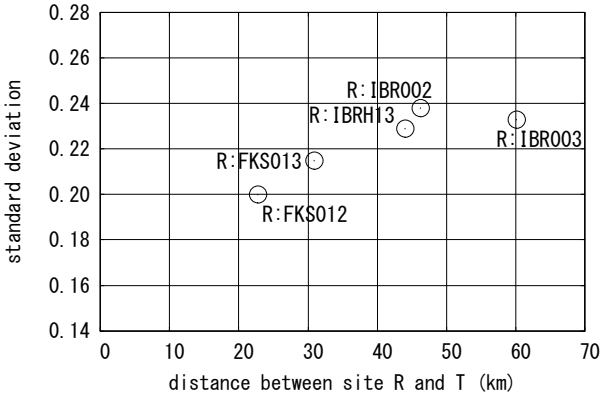

(1) T: FKS011

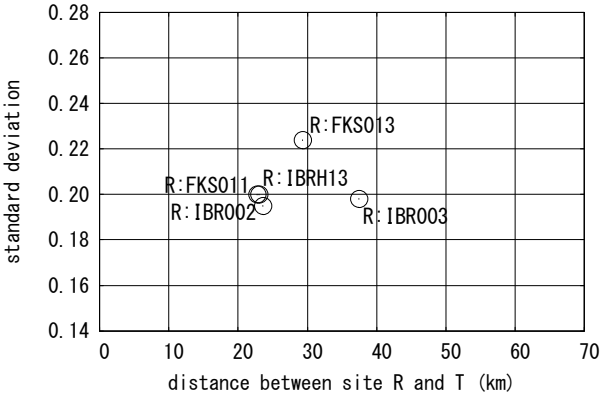

(2) T: FKS012

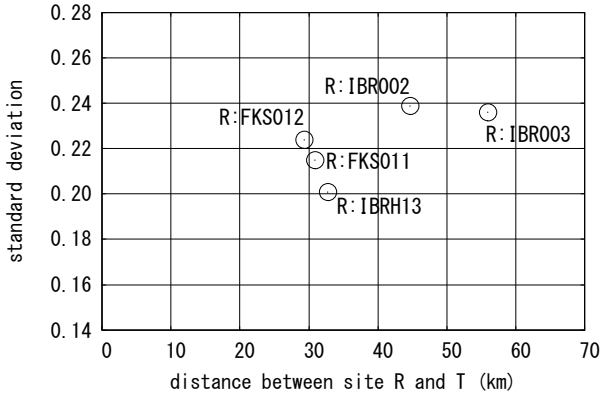

(3) T: FKS013

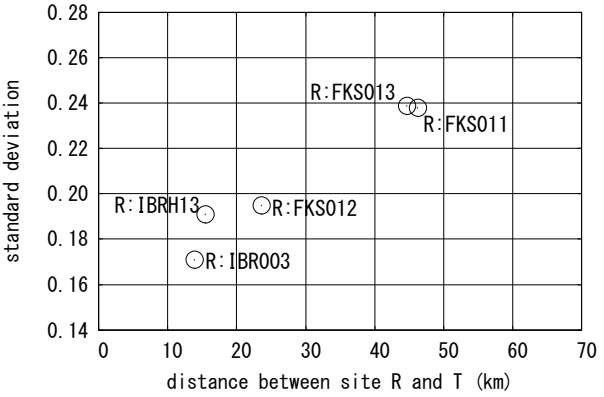

(4) T: IBR002

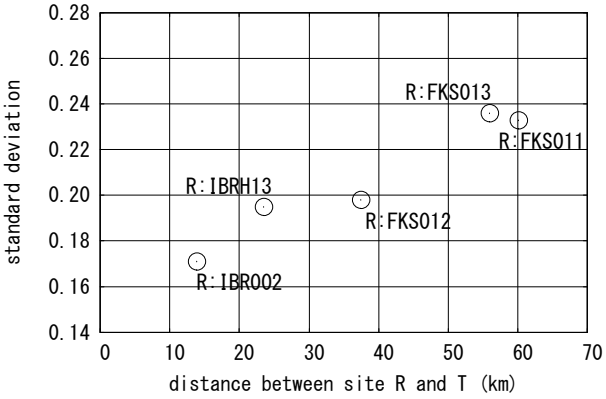

(5) T: IBR003

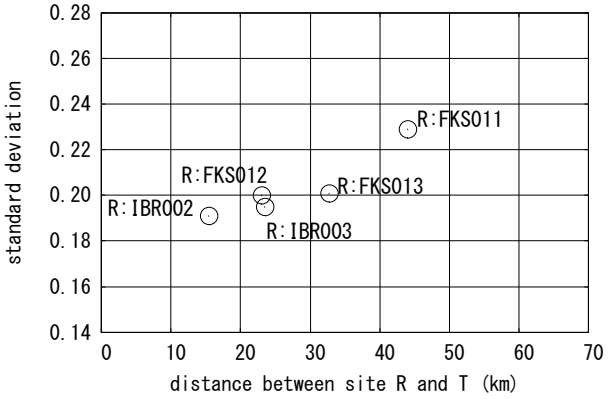

(6) T: IBRH13

Fig. 5 – Relationship between points distance and standard deviation of PSR (0.2 to 5 Hz average) (Case 1)

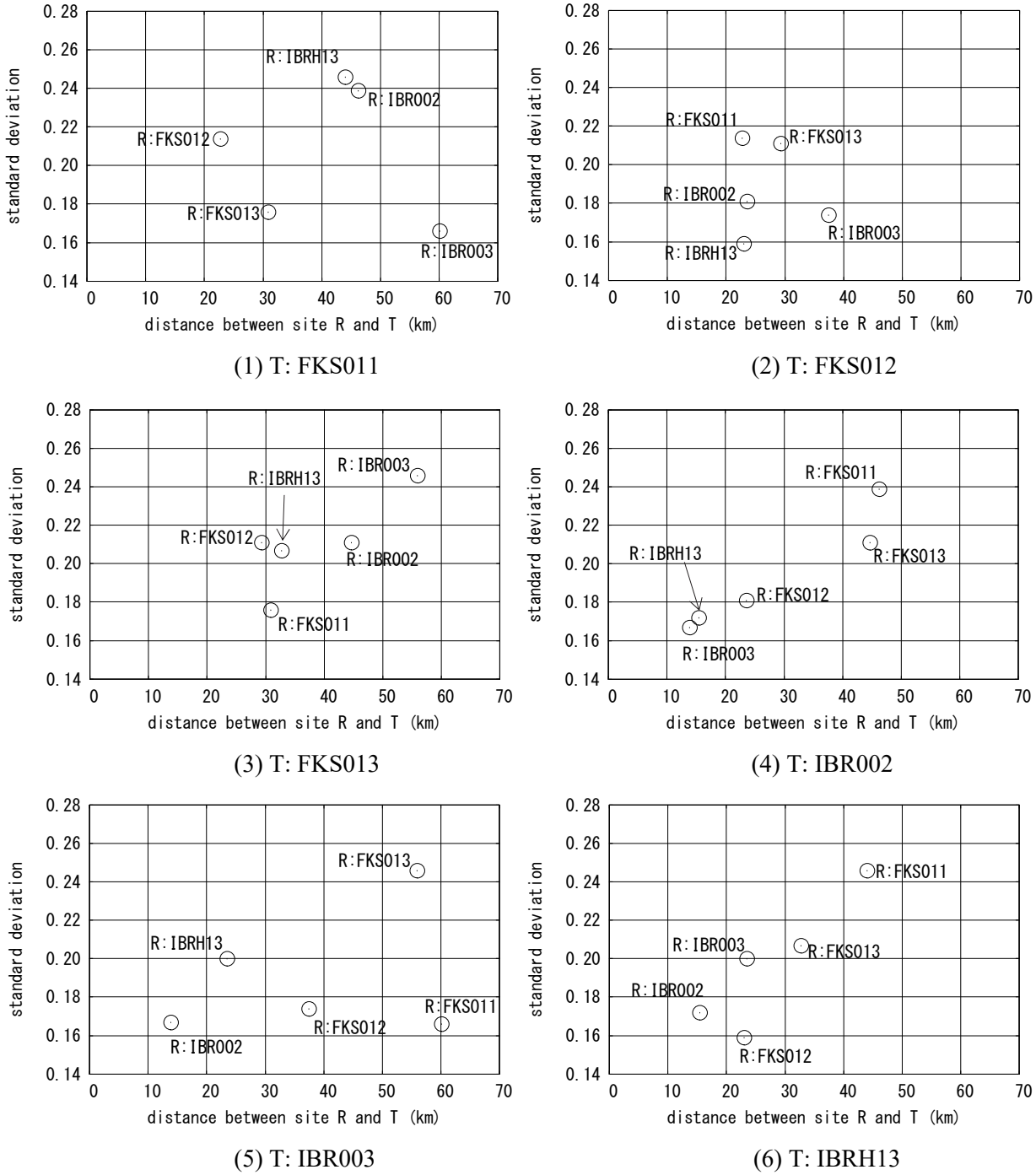

(1) T: FKS011 (2) T: FKS012

(3) T: FKS013 (4) T: IBR002

(5) T: IBR003 (6) T: IBRH13

Fig. 6 – Relationship between points distance and standard deviation of PSR (0.2 to 5 Hz average) (Case 2)

4. Conclusion

In this study, the dispersion of PSR was calculated on the basis of the intra-event Fourier spectral ratio using the simultaneous observation record taking six strong-motion earthquake observation points in Fukushima and Ibaraki Prefecture as an object. Two cases were studied: the case in which the hypocentral distance difference of the reference and target site is not limited, and the case in which the hypocentral distance to the reference and target site are limited to almost the same. As the result, the standard deviation of PSR tended to

increase in the former, when the distance between object points was large, while in the latter, the standard deviation of PSR did not show much dependence on the distance between object points.

For a point where the site amplification factor is unknown, estimation of the site amplification factor using the known site amplification factor of the neighboring point and the intra-event Fourier spectral ratio is often conducted in practical design to evaluate design waveform reflecting site-specific amplification factor. It is important to note that reference site shall be the neighboring site whose distance between the target site is small.

5. Acknowledgements

Authors would like to thank the National Research Institute for Earth Science and Disaster Prevention, Japan for providing the K-NET and KiK-net strong motion records.

6. References

[1] Nozu A, Nagao T and Yamada M (2008): A strong motion simulation method suitable for areas with less information on subsurface structure, *The 14th World Conference on Earthquake Engineering*, Beijing, China.

[2] Nozu A, and Nagao T (2005): Site amplification factors for strong-motion sites in Japan based on spectral inversion technique, Technical Note of the Port and Airport Research Institute, No.1102. (in Japanese)

[3] Nozu A, Nagao T and Yamada M (2006): Simulation of Strong Ground Motions Based on Site-Specific Amplification and Phase Characteristics, *Third International Symposium on the Effects of Surface Geology on Seismic Motion*, Grenoble, France.

[4] Petukhin A, Irikura K, Ohmi S, Kagawa T (2003): Estimation of q-values in the seismogenic and aseismic layers in the Kinki region, Japan, by elimination of the geometrical spreading effect using ray approximation, *Bulletin of the Seismological Society of America*, Vol. 93, No. 4, pp. 1498-1515.

[5] Fukushima Y and Nagao T (2019): Variation of Earthquake Ground Motions with Focus on Site Amplification Factors: A Case Study, *Engineering, Technology & Applied Science Research*, Vol. 9, No. 4, pp.4355-4360.

[6] Satoh T. and Tatsumi Y (2002): Source, path, and site effects for crustal and subduction earthquakes inferred from strong motion records in Japan, *J. Struct. Constr. Eng. AIJ*, Vol.556, pp.15-24. (in Japanese)

[7] Aki K (1967): Scaling law of seismic spectrum, *Journal of Geophysical Research*, Vol. 72, No. 4, pp. 1217-1231.

[8] Kinoshita S (1998): Kyoshin Net (K-NET), *Seism. Res. Lett.*, Vol.69, pp.309-332.

[9] Aoi S, Obara K, Hori S, Kasahara K, Okada Y (2000): New strong-motion observation network: KiK-net, *Eos Transactions American Geophysical Union*, Vol. 81.

[10] Fujiwara H, Kawai S, Hao KXS, Morikawa N, Azuma H (2017): J-SHIS An Integrated System for Sharing Information on National Seismic Hazard Maps for Japan, *16th World Conference on Earthquake Engineering*, Santiago, Chile.

[11] Japan Road Association (2015): A reference to specifications for highway bridges part 5, seismic design, Maruzen Co., Ltd. (in Japanese)

[12] Somerville PG. and Helmberger DV (1990): The effect of crustal structure on the attenuation of strong ground motion in eastern north America, *Proc. of Fourth U. S. National Conf. on Earthq. Eng.*, Vol.1, pp.385-394.

[13] Takahashi H, Hirai T, Fukuwa N (2015): Study on Relationship between Site Effects and Arrival Directions of Seismic Waves based on Ground Motion Records, *Summaries of Technical Papers of Annual Meeting Architectural Institute of Japan*, pp.47-48. (in Japanese)

[14] Nagao T, Yamada M, Nozu A (2009): The effect of the incident angle on the site amplification factors for deep basin structures by use of two-dimensional finite element analyses - For Osaka and Kushiro sedimentary basin -, *Journal of applied mechanics : JSCE*, Vol.12, pp.579-588. (in Japanese)

